

Three heavy jet events at hadron colliders as a sensitive probe of the Higgs sector

David Atwood

Department of Physics and Astronomy, Iowa State University, Ames, IA 50011, USA

Shaouly Bar-Shalom^y and Gad Eilam^z

Physics Department, Technion-Institute of Technology, Haifa 32000, Israel

Amrjit Soni^x

Theory Group, Brookhaven National Laboratory, Upton, NY 11973, USA

(Dated: November 4, 2021)

Assuming that a non-standard neutral Higgs with an enhanced Yukawa coupling to a bottom quark is observed at future hadron experiments, we propose a method for a better understanding of the Higgs sector. Our procedure is based on "counting" the number of events with heavy jets (where "heavy" stands for a c or b jet) versus b jets, in the final state of processes in which the Higgs is produced in association with a single high p_T c or b jet. We show that an observed signal of the type proposed, at either the Tevatron or the LHC, will rule out the popular two Higgs doublet model of type II as well as its supersymmetric version – the Minimal Supersymmetric Standard Model (MSSM), and may provide new evidence in favor of some more exotic multi-Higgs scenarios. As an example, we show that in a version of a two Higgs doublet model which naturally accounts for the large mass of the top quark, our signal can be easily detected at the LHC within that framework. We also find that such a signal may be observable at the upgraded Tevatron Run III, if the neutral Higgs in this model has a mass around 100 GeV and $\tan\beta > 50$ and if the efficiency for distinguishing a c jet from a light jet reaches the level of 50%.

PACS numbers: 12.15.Ji, 12.60.Fr, 12.60.-i, 14.80.Cp

I. INTRODUCTION

With the Tevatron Run II underway at Fermilab, the future Tevatron upgrade Run III and the Large Hadron Collider (LHC) at CERN, the discovery of the Higgs boson is currently believed to be "around the corner". These machines will be able to detect the neutral Higgs over its entire theoretically allowed mass range [1].

If the Higgs Yukawa coupling to a bottom quark is enhanced, as predicted for example in general multi-Higgs models and in the supersymmetric version of the two Higgs Doublet Model (2HDM) – the MSSM – when $\tan\beta$ is large, then the neutral Higgs may be produced at Leading Order (LO) through $b\bar{b}$ fusion $b\bar{b} \rightarrow h$ [2]. In such models, a sizable production rate of a neutral Higgs in association with b quark jets is also expected via the sub-processes $g b \rightarrow h b$ [3, 4] and $g q \rightarrow h q$ [5].^[1] In particular, as was shown in [3], if one demands that only one b jet will be produced (in association with the Higgs) at high p_T , then $g b \rightarrow h b$ becomes the LO and is therefore the dominant Higgs-bottom associated production mechanism for large $\tan\beta$. For example, $g b \rightarrow h b$ followed by $h \rightarrow b\bar{b}$ may already prove to be a useful probe of the

neutral Higgs sector at the Tevatron future runs [6].

In this work we assume that indeed the Higgs has an enhanced coupling to bottom quarks and that it will be therefore discovered or observed in association with bottom quarks jets, via one of the above production channels. Discovery of such a non-standard Higgs should start an exploration era of the various Higgs Yukawa couplings to fermions in order to decipher the origin and detailed properties of the Higgs sector. For that purpose, special observables should be devised that will enable the experimentalists to pin-down some specific Higgs Yukawa interactions. In particular, one should find observables which are sensitive to a specific Yukawa coupling or combination of couplings, and are therefore able to exclude models with an enhanced Higgs-bottom Yukawa vertex, or provide further evidence in favor of a definite Higgs scenario.

In this paper we follow this line of thought and present a method which is useful for an investigation of the relation between the Higgs-charm and Higgs-bottom Yukawa couplings. We focus on neutral Higgs production via a single high p_T charm or bottom jet, $q q \rightarrow q h$, $q = c$ or b , followed by $h \rightarrow b\bar{b}$ or $h \rightarrow c\bar{c}$.^[2] Our final state is therefore defined to be composed of exactly three non-light jets, where a light jet means a u ; d ; s or g (gluon) jet. If the Higgs is not the Standard Model (SM) one, par-

^xElectronic address: atwood@iastate.edu

^yElectronic address: shaouly@physics.technion.ac.il

^zElectronic address: eilam@physics.technion.ac.il

^xElectronic address: soni@bnl.gov

[1] Unless stated otherwise, h will be used to denote the neutral Higgs that drives the processes under consideration.

[2] We will not explicitly write the charge of the quarks involved. All charge-conjugate sub-processes are understood throughout this paper.

ticularly if the Higgs-bottom Yukawa is large, then this class of processes may play an important role in Higgs searches, discovery and characterization at hadron colliders.

Based on this type of production mechanism, we suggest an observable which is particularly sensitive to new physics in the ratio between the Higgs-charm and the Higgs-bottom Yukawa couplings. We find that our signal is insensitive to the Higgs sectors of the type II 2HDM (2HDM II) and of the MSSM. Therefore, a positive signal of our observable at either the Tevatron or the LHC will rule out these models. We also consider a different type of a 2HDM, the so called "2HDM for the top quark" (T2HDM), which is an interesting model designed to naturally accommodate the large mass of the top quark. This model may be viewed as an effective low energy theory wherein the Yukawa interactions mimic some high energy dynamics which generates both the top mass and the weak scale. The two scalar doublets could be composite, as in top-color models, and the Yukawa interactions could be the residual effect of some higher energy four-Fermi operators. Interestingly, for this T2HDM our signal is significantly enhanced. We thus show that if this version of a 2HDM underlies the Higgs sector, then our signal will be easily detected (to many standard deviations) at the LHC and may also be detected at the Tevatron if $\tan\beta$ is large enough and if the efficiency of tagging a c-jet as a heavy-jet is of O(50%).

The paper is organized as follows: in section II we define our signal. In section III we present the numerical setup and discuss the experimental background. In section IV we evaluate our signal in three different versions of a 2HDM and discuss the expectations from the T2HDM, the 2HDM II and the MSSM. In section V we summarize our results.

II. NOTATION AND DEFINITION OF THE SIGNAL

Let j_h denote a "heavy" b or c-quark jet. Specifically, a j_h jet should not be a u, d, s or gluon jet (i.e., with the veto $j_h \notin \{u; d; s; g\}$ jet). Let j_b be a b-quark jet. Clearly, every jet of type j_b is also a j_h . Likewise, let us denote by j_c a c-quark jet.

We thus define the cross-sections

$$\sigma(j_h j_h j_h) = (\text{pp or pp} \rightarrow j_h j_h j_h + X); \quad (1)$$

$$\sigma(j_b j_b j_b) = (\text{pp or pp} \rightarrow j_b j_b j_b + X); \quad (2)$$

and the ratio

$$R = \frac{\sigma(j_h j_h j_h)}{\sigma(j_b j_b j_b)}; \quad (3)$$

Note that, since j_h is either a j_b or a j_c , it follows that:

$$\sigma(j_h j_h j_h) = \sigma(j_b j_b j_b) + \sigma(j_c j_c j_c) + \sigma(j_b j_c j_c) + \sigma(j_c j_b j_c); \quad (4)$$

From the above definitions it is evident that:

$$R = 1 / \left(\frac{Y_c^2}{Y_b^2} + O\left(\frac{Y_c^4}{Y_b^4}\right) \right); \quad (5)$$

where Y_c and Y_b are the Higgs-charm and Higgs-bottom Yukawa couplings, respectively.

In reality, one has to include non-ideal efficiencies for jet identification. Therefore, we define the quantity ϵ_j^k to be the efficiency for identifying a j -jet as a k -jet. Thus, for example, ϵ_b^b or ϵ_b^h are the efficiencies for misidentifying a light-jet (j_l) as a b-jet (j_b) or as a heavy-jet (j_h), respectively. Using these efficiency factors we define the experimental observable as:

$$R^M = \frac{\sum_{j_b j_b j_b}^M}{\sum_{j_b j_b j_b}^M}; \quad (6)$$

where $R = \sigma(j_h j_h j_h) = \sigma(j_b j_b j_b)$ with $\sigma(j_h j_h j_h)$, $\sigma(j_b j_b j_b)$ being the effective signals for cross-sections that will actually be measured in the experiment and R^M is the value of R calculated within a specific Higgs model M via the sub-processes $gq \rightarrow qh \rightarrow qqq$, $q = \text{c or b}$. Thus, in the limit of an ideal detector where $\epsilon_j^k = \delta_j^k$, $R^M = R$ (where R^M means the "ideal" ratio defined in (3) calculated within model M). In particular, these cross-sections include all tagging efficiencies as follows:

$$\sum_{j_b j_b j_b}^M = \sum_{j_1 j_2 j_3}^M \epsilon_{j_1}^{b_b} \epsilon_{j_2}^{b_b} \epsilon_{j_3}^{b_b} \sigma(j_1 j_2 j_3); \quad (7)$$

$$\sum_{j_h j_h j_h}^M = \sum_{j_1 j_2 j_3}^M \epsilon_{j_1}^{h_h} \epsilon_{j_2}^{h_h} \epsilon_{j_3}^{h_h} \sigma(j_1 j_2 j_3); \quad (8)$$

In the limit $(Y_c/Y_b)^2 \rightarrow 0$, one obtains

$$R^M \rightarrow R^0 = \frac{\sum_{j_b j_b j_b}^M}{\sum_{j_b j_b j_b}^M} \xrightarrow{Y_c/Y_b \rightarrow 0} \frac{(\epsilon_b^h)^3 \sum_{j_b j_b j_b}^M}{(\epsilon_b^b)^3 \sum_{j_b j_b j_b}^M} = \frac{\epsilon_b^h^3}{\epsilon_b^b^3}; \quad (9)$$

Therefore, due to the non-ideal efficiencies (in particular if $\epsilon_b^h \neq \epsilon_b^b$), we have $R^0 \neq 1$ even if the Higgs Yukawa coupling to the charm quark is negligible. As will be shown below, this limit is applicable to a neutral Higgs either of MSSM or of 2HDM II origin, if $\tan\beta$ is large. That is, for large $\tan\beta$

$$R^{\text{MSSM}}; R^{2\text{HDM II}} \rightarrow R^0 = \frac{\epsilon_b^h^3}{\epsilon_b^b^3}; \quad (10)$$

A deviation from $R^M = R^0$, indicating a high rate for $h \rightarrow cc$, signals a specific type of new physics in the Higgs

sector, e.g., beyond the MSSM or the 2HDM Higgs scenario. Such a deviation is parameterized by:

$$R^M = R^M - R^0 / \frac{Y_c}{Y_b}^2 + O\left(\frac{Y_c}{Y_b}^4\right); \quad (11)$$

The significance with which R^M can be measured depends on the experimental error R_{exp}^M :

$$R_{\text{exp}}^M = R^M \sqrt{\frac{S}{\frac{(N_{j_h j_h j_h}^M)^2}{(N_{j_h j_h j_h}^M)^2} + \frac{(N_{j_b j_b j_b}^M)^2}{(N_{j_b j_b j_b}^M)^2}}}; \quad (12)$$

where $N_{j_h j_h j_h}^M = \frac{M}{j_h j_h j_h} L$ and similarly for $N_{j_b j_b j_b}^M$, with L being the integrated luminosity at the given collider. The errors in the measurements of $N_{j_h j_h j_h}^M$ and $N_{j_b j_b j_b}^M$ are (statistical only): $N_{j_h j_h j_h}^M = \frac{M}{j_h j_h j_h} \sqrt{N_{j_h j_h j_h}^M}$ and $N_{j_b j_b j_b}^M = \frac{M}{j_b j_b j_b} \sqrt{N_{j_b j_b j_b}^M}$, where $N_{j_h j_h j_h}$ and $N_{j_b j_b j_b}$ (i.e., without the superscript M) are the total number of events dominated by the background processes.

Eq.(12) can be simplified to:

$$R_{\text{exp}}^M = \frac{M \sqrt{N_{j_h j_h j_h}^M + (R^M)^2 N_{j_b j_b j_b}^M}}{N_{j_b j_b j_b}^M}; \quad (13)$$

therefore, since $N_{j_b j_b j_b}^M / Y_b^2$, it follows that $R_{\text{exp}}^M / 1 = Y_b^2$. In particular, if $Y_b / \tan \beta$, then $R_{\text{exp}}^M / 1 = \tan^2 \beta$.

The condition, $R^M > R_{\text{exp}}^M$ signals that new physics in the ratio between the hcc and hbb Yukawa couplings can be seen, with a statistical significance of

$$N_{SD} = \frac{R^M}{R_{\text{exp}}^M}; \quad (14)$$

III. NUMERICAL SETUP AND BACKGROUND

Before presenting our results let us describe the numerical setup:

All signal and background cross-sections are calculated at leading order (tree-level), using the COM-PHEP package [7] with the CTEQ5L [8] parton distribution functions.

Throughout our entire analysis to follow, the following set of cuts are employed in both signal and background cross-sections:

1. For both the Tevatron and the LHC, in order for the jets to be within the tagging region of the silicon vertex detector, we require all three jets to have the following minimum transverse momentum (p_T) and rapidity (y) coverages:

Tevatron: $p_T(j) > 15 \text{ GeV}$; $y(j) < 2$,
LHC: $p_T(j) > 30 \text{ GeV}$; $y(j) < 2.5$,
where j is any of the three jets in the final state.

2. The signal cross-sections always have one pair of jets (coming from the Higgs decay) that should reconstruct the Higgs mass. Thus, in order to improve the signal to background ratio, we require for both the signal and background cross-sections that only one jet pair (out of the three possible jet pairs in the final state), will have an invariant mass within $m_h - 0.05m_h$, i.e., within 5% of m_h around m_h . That is, we reject events if the invariant masses of more than one $j_i j_k$ pair are within $m_h - 0.05m_h < M_{j_i j_k} < m_h + 0.05m_h$. This acceptance cut is found to significantly improve the signal to background ratio.
3. We impose a common lower cut on the invariant masses of all three jet pairs: $M_{j_i j_k} > m_h = 2$. This additional cut further improves the signal to background ratio.
4. We require the final state partons to be separated by a cone angle of $R > 0.7$, where here R stands for $\sqrt{p_{\perp 1}^2 + p_{\perp 2}^2}$.

We use the $\overline{\text{MS}}$ running Yukawa couplings $Y_b(R) / (m_b(R)=v)$, $Y_c(R) / (m_c(R)=v)$, where $m_b(R)$ and $m_c(R)$ are $\overline{\text{MS}}$ running masses. We take a renormalization scale of $R = m_h$ as our central value. In particular, $m_b(m_h)$ and $m_c(m_h)$ are calculated via the next-to-leading-order heavy quark $\overline{\text{MS}}$ running mass equation [9], using $m_b(m_b)$ and $m_c(m_c)$ as the initial conditions. This brings up some uncertainty corresponding to the allowed range of $m_b(m_b)$ and $m_c(m_c)$: $4 \text{ GeV} < m_b(m_b) < 4.5 \text{ GeV}$ and $1 \text{ GeV} < m_c(m_c) < 1.4 \text{ GeV}$, see [10]. In what follows we use $m_b(m_b) = 4.26 \text{ GeV}$ and $m_c(m_c) = 1.26 \text{ GeV}$ as our central values [10], which give the $m_b(m_h)$ and $m_c(m_h)$ masses listed in Table I.

TABLE I: Running charm and bottom quark $\overline{\text{MS}}$ (NLO) masses at $R = m_h$ for $m_h = 100; 120$ and 140 GeV , with the initial conditions $m_b(m_b) = 4.26 \text{ GeV}$ and $m_c(m_c) = 1.26 \text{ GeV}$.

running charm and bottom $\overline{\text{MS}}$ masses $m_b(m_b) = 4.26 \text{ GeV}$, $m_c(m_c) = 1.26 \text{ GeV}$			
+ [GeV]	$R = 100$	$R = 120$	$R = 140$
$m_b(R)$	2.94	2.89	2.86
$m_c(R)$	0.61	0.6	0.59

At some instances we will refer to the "maximal signal" possible. This means that we are evaluating the signal cross-sections with the initial conditions $m_b(m_b) = 4.5 \text{ GeV}$ and $m_c(m_c) = 1.4$

GeV, i.e., at their upper allowed values, which at $m_R = 100$ GeV gives: $m_b(100 \text{ GeV}) = 3.1 \text{ GeV}$ and $m_c(100 \text{ GeV}) = 0.68 \text{ GeV}$.

Unless stated otherwise, the parton distribution functions are evaluated with a factorization scale of $\mu_F = m_h$. Thus, we use a common factorization and renormalization scale $\mu_F = \mu_R$ and take $\mu_F = m_h$ as our nominal value. The uncertainty of our signal cross-sections, obtained by varying the factorization scale μ_F about its central value ($\mu_F = m_h$) within the range $m_h/4 < \mu_F < 2m_h$, will also be investigated.

We do not consider the next-to-leading-order (NLO) contributions to $(gg \rightarrow qh)$. As was shown in [3], the NLO contribution to $(bg \rightarrow bh)$ can amount to an effective K -factor of about 1.5 at the Tevatron and about 1.2 at the LHC. Assuming that a similar K -factor applies also to $(cg \rightarrow ch)$, our signal R^M is essentially insensitive to the NLO corrections since it involves ratios of these cross-sections. Moreover, R_{exp}^M is proportional to $\sqrt{K^B} = K^S$, where K^B and K^S are the K -factors for the background and the signal three jets events, respectively. Thus, at NLO, the statistical significance of our signal ($N_{SD} = R^M = R_{\text{exp}}^M$) should be about a factor of $K^S = \sqrt{K^B}$ larger or smaller than our tree-level estimate, depending on the size of K^B and K^S . For $K^B = K^S > 1$, our tree-level prediction for N_{SD} is on the conservative side.

Since we require our signal to be composed out of events with exactly three jets in the final state (i.e., 3 heavy jets, $j_h j_h j_h$), we do not consider processes with 4 heavy jets or 4 b jets in the final state, e.g., $gg; qq \rightarrow bbb; bbbb$. These type of sub-processes constitute a partial source of the K factor for the 3 heavy jets signal cross-sections [3]. Moreover, as was further demonstrated in [3] for the case of Higgs-bottom associated production at hadron colliders, even if we had relaxed our demand for exactly 3 jets in the final state to allow for 3 or 4 jets with 3 or 4 jet tags, the contribution of events with 4 jets to R^M would still constitute no more than 10% of those with exactly 3 jets in the final state.

Let us now discuss the background cross-sections. The irreducible background for the various three heavy jet final states, $j_h j_h j_h$ with $h = c$ or b , is dominated by the QCD sub-processes $bg \rightarrow bg; bbb; bcc$ and $cg \rightarrow cg; ccc; cbb$. Other processes like Z production followed by its decay, $bg \rightarrow bZ; bbb; bcc$ and $cg \rightarrow cZ; ccc; cbb$, and QED also contribute to the background. In what follows, this irreducible background is calculated using the COMPHEP package [7], where all possible tree-level diagrams (QCD, Electroweak and QED) for the $j_h j_h j_h$ final state are included. In addition, due to the non-ideal

efficiencies, e.g., the non-zero probability of misidentifying a light jet for a heavy jet, there is a reducible background for the three heavy jet final states coming from sub-processes in which one, two or all three jets are light. Since one expects that $\frac{h}{l}; \frac{b}{l}; \frac{h}{b}; \frac{b}{b}; \frac{h}{c}; \frac{b}{c}$ (see e.g., [11]), the reducible background cross-sections, when multiplied by $\frac{h}{l}$ or $\frac{b}{l}$ are dominated by processes in which only one jet out of the three is light. Moreover, we find that, at both the Tevatron and the LHC, the one-light-jet reducible background is by far controlled by the $gg \rightarrow gbb$ and $gg \rightarrow gcc$ sub-processes, which will be therefore included in our background estimation. For example, the contribution of $gg \rightarrow gbb$ to the $j_h j_h j_h$ final state is: $\frac{B}{j_h j_h j_h} = gg \rightarrow gbb \frac{h}{l} (\frac{h}{b})^2$ (the background signals will always be denoted by the superscript B).

In Tables II and III we list the background cross-sections at the Tevatron and at the LHC, respectively, where all cross-sections are calculated with the set of cuts 1-4, described earlier. The background cross-sections are calculated with a factorization scale set to $\mu_F = \sqrt{s}$, where \sqrt{s} is the square of the cm. energy of the hard cross-sections.

TABLE II: Background cross-sections in [fb], for the Tevatron with a cm. of $\sqrt{s} = 2 \text{ TeV}$. All cross-sections are calculated with the following kinematical cuts (some defined as a function of m_h): (1) $p_T(j) > 15 \text{ GeV}$, (2) $j_j j_j < 2$, where j is any (heavy and light) of the three jets in the final state, (3) the acceptance cut that the invariant mass of only one jet pair $M_{j_i j_k}$, $i \neq k$, out of the three possible pairs of jets in the final state is within the mass range $(m_h - 0.05 m_h) < M_{j_i j_k} < (m_h + 0.05 m_h)$, (4) $M_{j_i j_k} > m_h/2$, for all three jet pairs, and (5) any two partons in the final state are separated by a cone of $R > 0.7$. Numbers are rounded to the 1% accuracy as was obtained from the COMPHEP numerical sessions.

Background cross-sections at the Tevatron			
[fb] / [GeV]	m_h used for the kinematical cuts		
	$m_h = 100$	$m_h = 120$	$m_h = 140$
$\frac{B}{j_h j_h j_h} (gb \rightarrow bbb \text{ or } bcc)$	4.4 $\cdot 10^1$	1.8 $\cdot 10^1$	9.5 $\cdot 10^1$
$\frac{B}{j_h j_h j_h} (gc \rightarrow cbb \text{ or } ccc)$	7.2 $\cdot 10^1$	3.0 $\cdot 10^1$	16.3 $\cdot 10^1$
$\frac{B}{j_h j_h j_h} (gg \rightarrow gbb \text{ or } gcc)$	230 $\cdot 10^1$	94 $\cdot 10^1$	41 $\cdot 10^1$

TABLE III: Background cross-sections in [fb], for the LHC with a cm. of $\sqrt{s} = 14 \text{ TeV}$. All cross-sections are calculated with $p_T(j) > 30 \text{ GeV}$, $j_j j_j < 2.5$ and the additional kinematical cuts 3-5 as in Table II (see caption to Table II).

Background cross-sections at the LHC			
[fb] / [GeV]	m_h used for the kinematical cuts		
	$m_h = 100$	$m_h = 120$	$m_h = 140$
$\frac{B}{j_h j_h j_h} (gb \rightarrow bbb \text{ or } bcc)$	133 $\cdot 10^1$	111 $\cdot 10^1$	84 $\cdot 10^1$
$\frac{B}{j_h j_h j_h} (gc \rightarrow cbb \text{ or } ccc)$	190 $\cdot 10^1$	159 $\cdot 10^1$	120 $\cdot 10^1$
$\frac{B}{j_h j_h j_h} (gg \rightarrow gbb \text{ or } gcc)$	5680 $\cdot 10^1$	4720 $\cdot 10^1$	3540 $\cdot 10^1$

IV. EXPECTATIONS FROM TWO HIGGS DOUBLET MODELS

The signal cross-sections depend on the Higgs couplings and therefore on the underlying Higgs model. In what follows we will investigate the sensitivity of our signal R^M to various versions of a 2HDM.

The most general 2HDM Yukawa term is given by

$$L_Y = \sum_{i,j} Q_L^i \left(U_{ij}^1 \tilde{\sim}_1 + U_{ij}^2 \tilde{\sim}_2 \right) u_R^j + D_{ij}^1 \tilde{\sim}_1 + D_{ij}^2 \tilde{\sim}_2 d_R^j ; \quad (15)$$

where Q_L is the SU(2) left-handed quark doublet, u_R and d_R are the right-handed up and down quark SU(2) singlets, respectively, and $\tilde{\sim}_{1,2} = i_{2-1,2}$. Also, $U^1; U^2; D^1; D^2$ are general Yukawa 3×3 matrices in flavor space. The different types of 2HDM's are then categorized according to the different choices of the Yukawa matrices $U^1; U^2; D^1; D^2$.

A. The 2HDM for the top quark - T2HDM

As an example of a Higgs sector that can give rise to an observable effect via R^M , we consider first the so called "2HDM for the top", in which the top quark receives a special status [12]. We will denote this model by T2HDM. In the T2HDM one defines [12]

$$\begin{aligned} U_{ij}^1 &= G_{ij} \quad (j_1 + j_2) ; \\ U_{ij}^2 &= G_{ij} \quad j_3 ; \\ D_{ij}^2 &= 0 ; \end{aligned} \quad (16)$$

where G is an unknown Yukawa 3×3 matrix in quark flavor space. The large mass of the top is, thus, naturally accommodated in the T2HDM by coupling the second Higgs doublet (ϕ_2), which has a much larger Vacuum Expectation Value (VEV), only to the top quark. This model has therefore large $\tan \beta = v_2/v_1$ by construction. That is, v_2 is the VEV responsible for the top quark mass, while v_1 generates the masses of all the other quarks.

Like any other 2HDM, the Higgs spectrum of the T2HDM is composed out of three neutral Higgs; two CP-even scalars and one pseudoscalar, and a charged Higgs. Choosing the basis $\phi = \phi_1$, where ϕ is the usual mixing angle between the two CP-even Higgs particles (see e.g., [13]), the neutral Higgs spectrum of the T2HDM is rotated such that it contains a SM-like neutral Higgs, H_{SM} , (with the SM couplings to fermions), a CP-even Higgs, h , and a pseudoscalar (CP-odd Higgs), A . The Yukawa couplings of h and A to down and up-type quarks in the T2HDM are:

$$\begin{aligned} hdd &: Y_d^{SM} \tan \beta ; \\ huu &: Y_u^{SM} \tan \beta ; u = u \text{ or } c ; \\ htt &: Y_t^{SM} \cot \beta ; \\ Add &: Y_d^{SM} \tan \beta ; \\ Auu &: Y_u^{SM} \tan \beta ; u = u \text{ or } c ; \\ Att &: Y_t^{SM} \cot \beta ; \end{aligned} \quad (17)$$

where $d = d; s \text{ or } b$ and $Y_f^{SM} = m_f/v$, $v = \sqrt{v_1^2 + v_2^2} = 246 \text{ GeV}$.

We therefore see that while the Yukawa couplings of h and A to down quarks in the T2HDM have the same pattern as in the 2HDM II and the MSSM, i.e., $Y_d / Y_d^{SM} \tan \beta$, their Yukawa couplings to u and c quark exhibit a different behavior, due to the special structure of the T2HDM's Yukawa matrices in (16). In particular, Y_c and Y_u are enhanced in the T2HDM by a factor of $\tan^2 \beta$ as compared to their values in the 2HDM II or in the MSSM, in which $Y_u / Y_u^{SM} \cot \beta$ for $u = u; c$ or t . Notice also that Y_t (in the T2HDM) remains the same as in the 2HDM II and the MSSM.

Therefore, as will be shown below, since $R^M / (Y_c/Y_b)^2$ [see (11)], we can expect to have the following relations: $R^{T2HDM} \propto R^{SM} / (m_c/m_b)^2$ and $R^{2HDM II}; R^{MSSM} \propto R^{T2HDM}$, when $\tan \beta$ is large. Note that in spite of the fact that $R^{SM} \propto R^{T2HDM}$, due to the small production rate of a SM (or a SM-like) Higgs via the gluon-b and gluon-c fusion channels, R^{SM} is overwhelmed by the very large background (i.e., R_{exp}^{SM}) and is thus unobservable.

In Tables IV and V we give the signal cross-sections at the Tevatron and at the LHC, respectively, for the T2HDM with $\tan \beta = 30$ and evaluated at $\sqrt{s} = m_h$ as the central value. To appreciate the uncertainties corresponding to variations of the factorization scale (μ_F), we also give in Tables IV and V the signal cross-sections evaluated with $\mu_F = m_h/4$ (upper uncertainty) and with $\mu_F = 2m_h$ (lower uncertainty), while keeping a fixed renormalization scale $\mu_R = m_h$. The effect of μ_F on the statistical significance of the signal will be discussed below.

All cross-sections in Tables IV and V are calculated with the set of cuts, as described in the previous section.^[3] To a good approximation, the signal cross-sections given in Tables IV and V are essentially insensitive to whether the Higgs produced is h or the pseudoscalar A . The difference between the two is the 1 versus the 5 couplings to fermions, which amounts to sign differences in the sub-leading terms involving m_b or m_c .

Using eqs. (6)-(8) and (13), (14), we plot in Figs. 1 and 2 the statistical significance (N_{SD}) of R^{T2HDM} (the

[3] The relevant Lagrangian pieces of the T2HDM were implemented into COMPHENP. Also, the Higgs width was explicitly calculated within the T2HDM via COMPHENP.

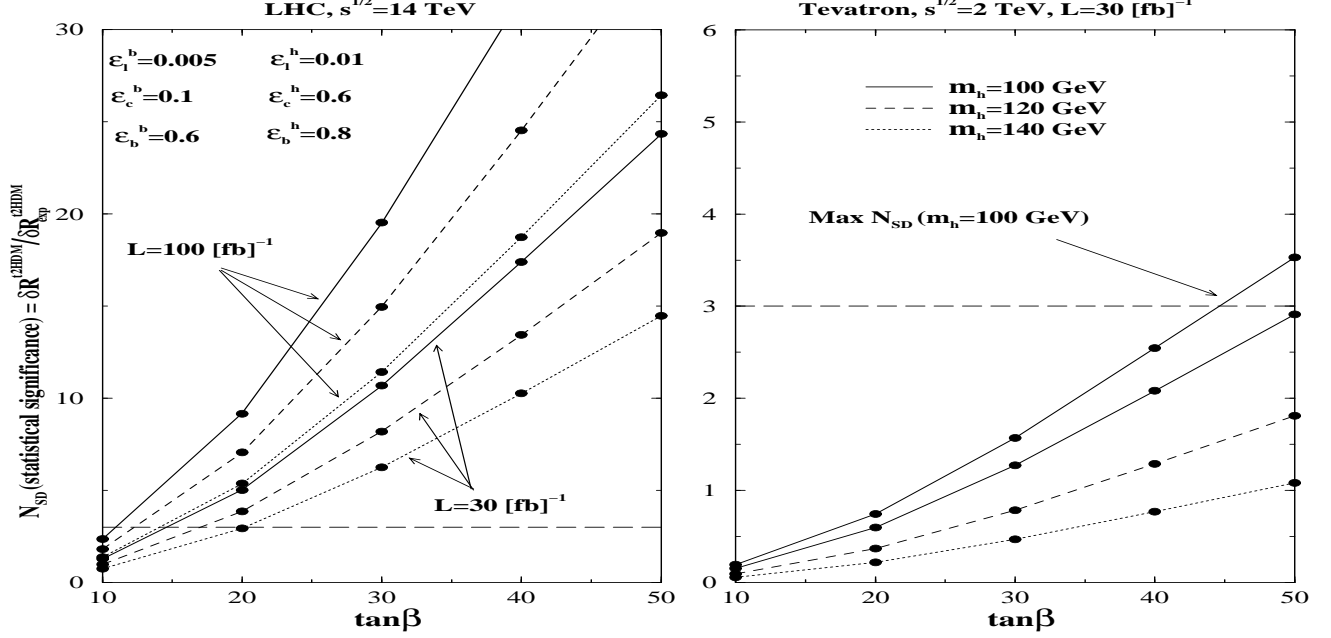


FIG. 1: The statistical significance of the signal in the T2HDM ($N_{SD} = R^{T2HDM} = R_{exp}^{T2HDM}$) as a function of $\tan\beta$ and for $m_h = 100; 120$ and 140 GeV, at the LHC with integrated luminosity of 30 fb^{-1} and 100 fb^{-1} (left plot) and at the Tevatron with integrated luminosity of 30 fb^{-1} (right plot). The upper solid curve on the right plot is for the case of maximal charm and bottom $M\bar{S}$ quark masses at $m_R = m_h = 100$ GeV (see discussion in section III). All cross-sections were calculated for $\mu_F = \mu_R = m_h$ and with the set of cuts 1-4 as outlined in section III.

TABLE IV: Signal cross-sections in [fb], for the T2HDM with $\tan\beta = 30$, at the Tevatron with a c.m. of $\sqrt{s} = 2$ TeV. All cuts are the same as for the background cross-sections at the Tevatron (see caption to Table II). The upper and lower uncertainties correspond to $\mu_F = m_h = 4$ and $\mu_F = 2m_h$, respectively.

Signal cross-sections for the T2HDM with $\tan\beta = 30$			
[fb] / [GeV]	Tevatron, $\sqrt{s} = 2$ TeV		
	$m_h = 100$	$m_h = 120$	$m_h = 140$
T2HDM (gb ! bbb)	$970^{+9\%}_{-9\%}$	$385^{+15\%}_{-10\%}$	$166^{+20\%}_{-12\%}$
T2HDM (gb ! bcc)	$42^{+9\%}_{-9\%}$	$16.6^{+15\%}_{-10\%}$	$7^{+20\%}_{-12\%}$
T2HDM (gc ! dbb)	$72^{+35\%}_{-14\%}$	$28.4^{+39\%}_{-15\%}$	$12.1^{+42\%}_{-15\%}$
T2HDM (gc ! ooc)	$3.1^{+35\%}_{-14\%}$	$1.23^{+39\%}_{-15\%}$	$0.52^{+42\%}_{-15\%}$

signal within the T2HDM), as a function of $\tan\beta$ for the LHC with an integrated luminosity of 30 fb^{-1} and 100 fb^{-1} and for the Tevatron with an integrated luminosity of 30 fb^{-1} . The statistical significance was calculated for $\tan\beta = 10; 20; 30; 40; 50$ and interpolation was employed to obtain the results for other values of $\tan\beta$. As our nominal values, the following efficiency factors

TABLE V: Signal cross-sections in [fb], for the T2HDM with $\tan\beta = 30$, at the LHC with a c.m. of $\sqrt{s} = 14$ TeV. All cuts are the same as for the background cross-sections at the LHC. See also captions to Table III and IV.

Signal cross-sections for the T2HDM with $\tan\beta = 30$			
[fb] / [GeV]	LHC, $\sqrt{s} = 14$ TeV		
	$m_h = 100$	$m_h = 120$	$m_h = 140$
T2HDM (gb ! bbb)	$46000^{+18\%}_{-1\%}$	$32400^{+12\%}_{-2\%}$	$21900^{+9\%}_{-1\%}$
T2HDM (gb ! bcc)	$2000^{+18\%}_{-1\%}$	$1400^{+12\%}_{-2\%}$	$940^{+9\%}_{-1\%}$
T2HDM (gc ! dbb)	$3050^{+0\%}_{-4\%}$	$2120^{+5\%}_{-3\%}$	$1400^{+7\%}_{-5\%}$
T2HDM (gc ! ooc)	$131^{+0\%}_{-4\%}$	$92^{+5\%}_{-3\%}$	$60^{+7\%}_{-5\%}$

were chosen [11]: $\epsilon_1^b = 0.005$, $\epsilon_1^h = 0.01$, $\epsilon_c^b = 0.1$, $\epsilon_b^b = 0.6$, $\epsilon_b^h = 0.3$, with $\epsilon_c^h = 0.6$ in Fig. 1 and $\epsilon_c^h = 0.3$ in Fig. 2.

Evidently, R^{T2HDM} can be easily observed at the LHC for $m_h = 100 \text{--} 140$ GeV, with a significance of more than 3-sigma for $\tan\beta = 0(20)$ if $\epsilon_c^h = 0.6$ and for $\tan\beta = 0(35)$ if $\epsilon_c^h = 0.3$. For example, already at the low luminosity stage of the LHC, i.e., with $L = 30 \text{ fb}^{-1}$, a 5-sigma detection of R^{T2HDM} will be obtained for

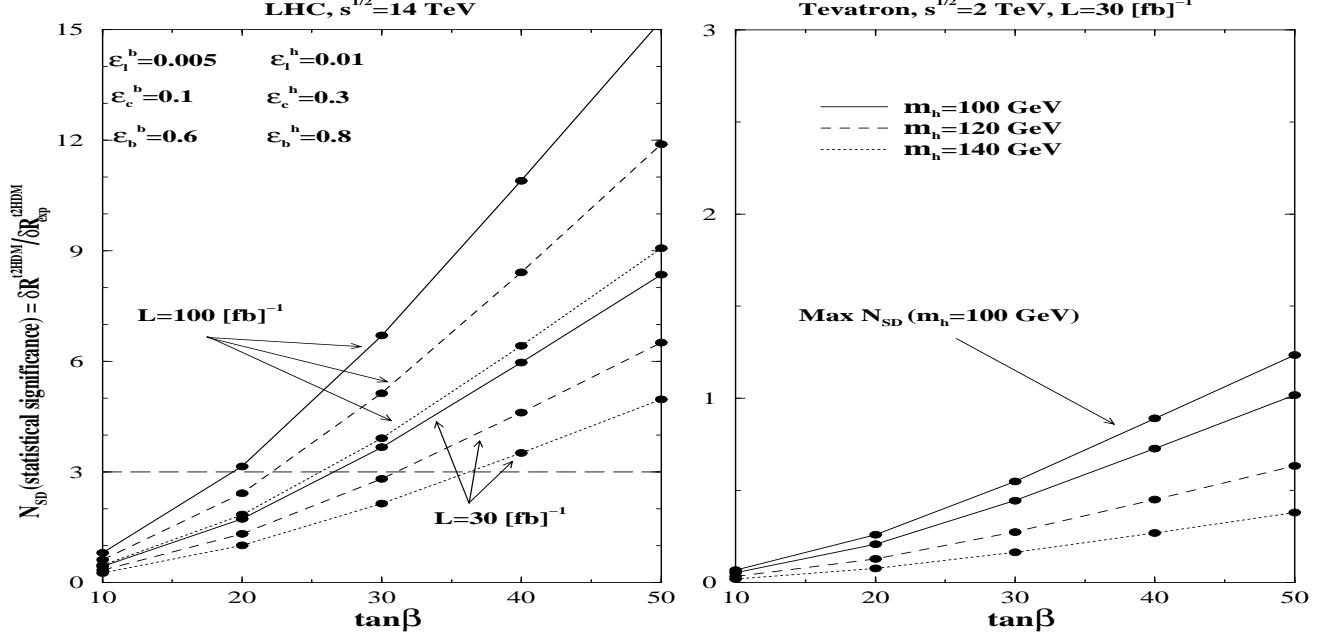


FIG. 2: Same as Fig. 1, for $h_c = 0.3$.

$m_h = 100$ GeV if $h_c = 0.6$ and $\tan \beta = 20$ or if $h_c = 0.3$ and $\tan \beta = 35$. On the other hand, a 3-sigma detection of R^{T2HDM} will be possible at the Tevatron only if $h_c > 0.5$ and if m_h is around 100 GeV and $\tan \beta > 50$. The maximal signal case [obtained when $m_b(m_h)$ and $m_c(m_h)$ are evaluated with maximal $m_b(m_h)$ and $m_c(m_h)$ as initial conditions, see the discussion in section III], is expected to give a 3-sigma effect at the Tevatron for $m_h = 100$ GeV and $\tan \beta > 45$ and if $h_c = 0.6$.

In Figs. 3 and 4 we give scatter plots which show the region in the h_b^h - h_c^h plane that will allow a 3-sigma detection of R^{T2HDM} at the LHC when $\tan \beta = 20$, $m_h = 100$ - 140 GeV, $b_1 = 0.005$, $h_1 = 0.01$, $b_c = 0.1$, and with a b-jet tagging efficiency of $b_b = 0.6$ in Fig. 3 or of $b_b = 0.4$ in Fig. 4. Clearly, a 3-sigma detection of R^{T2HDM} over the entire m_h mass range shown, will be possible at the LHC for a b-tagging efficiency of 60% ($b_b = 0.6$) [11] and with h_b^h ; h_c^h as low as 0.3 - 0.4 if $L = 100 \text{ fb}^{-1}$, or with h_b^h ; $h_c^h = 0.5$ - 0.6 if $L = 30 \text{ fb}^{-1}$. Fig. 4 shows that for a lower b-tagging efficiency of $b_b = 0.4$, the requirements of h_b^h ; $h_c^h > 0.4$ for $L = 100 \text{ fb}^{-1}$ and h_b^h ; $h_c^h > 0.6$ for $L = 30 \text{ fb}^{-1}$, will also suffice for a 3-sigma detection.

Finally, in Table VI we show the variation of the statistical significance of the signal (N_{SD} of R^{T2HDM}) for different choices of the factorization scale, $F = m_h = 4$; m_h and $2m_h$. The numbers in Table VI correspond to the LHC with an integrated luminosity of 100 fb^{-1} and are given for $\tan \beta = 30$. Evidently, only mild changes (smaller than 5%) in N_{SD} are obtained when varying the factorization scale within the range $m_h = 4$ - $F = 2m_h$.

TABLE VI: Comparison of the statistical significance in the T2HDM ($N_{SD} = R^{T2HDM} = R_{exp}^{T2HDM}$) for three values of the factorization scale $F = m_h = 4$; m_h and $2m_h$. N_{SD} is given for $m_h = 100$; 120 and 140 GeV and $\tan \beta = 30$, at the LHC with an integrated luminosity of 100 fb^{-1} .

N_{SD} in the T2HDM with $\tan \beta = 30$			
[GeV]	LHC with $L = 100 \text{ fb}^{-1}$		
	$m_h = 100$	$m_h = 120$	$m_h = 140$
$F = m_h = 4$	6.37	5.15	4.03
$F = m_h$	6.71	5.14	3.92
$F = 2m_h$	6.51	5.03	3.77

B. The 2HDM II and the MSSM

Let us now examine the expected signals $R^{2HDM II}$ and R^{MSSM} in the 2HDM II and in the MSSM, respectively. Here too, we assume from the outset that $\tan \beta$ is large enough so that the non-standard Higgs can be observed in association with bottom quark jets at the hadron colliders under investigation (recall that if the neutral Higgs does not have the necessary $\tan \beta$ enhancement in its Yukawa coupling to the bottom quark, then our signal ceases to be effective). Thus, in what follows we will focus only on the large $\tan \beta$ case.

The 2HDM II Yukawa couplings follow from the

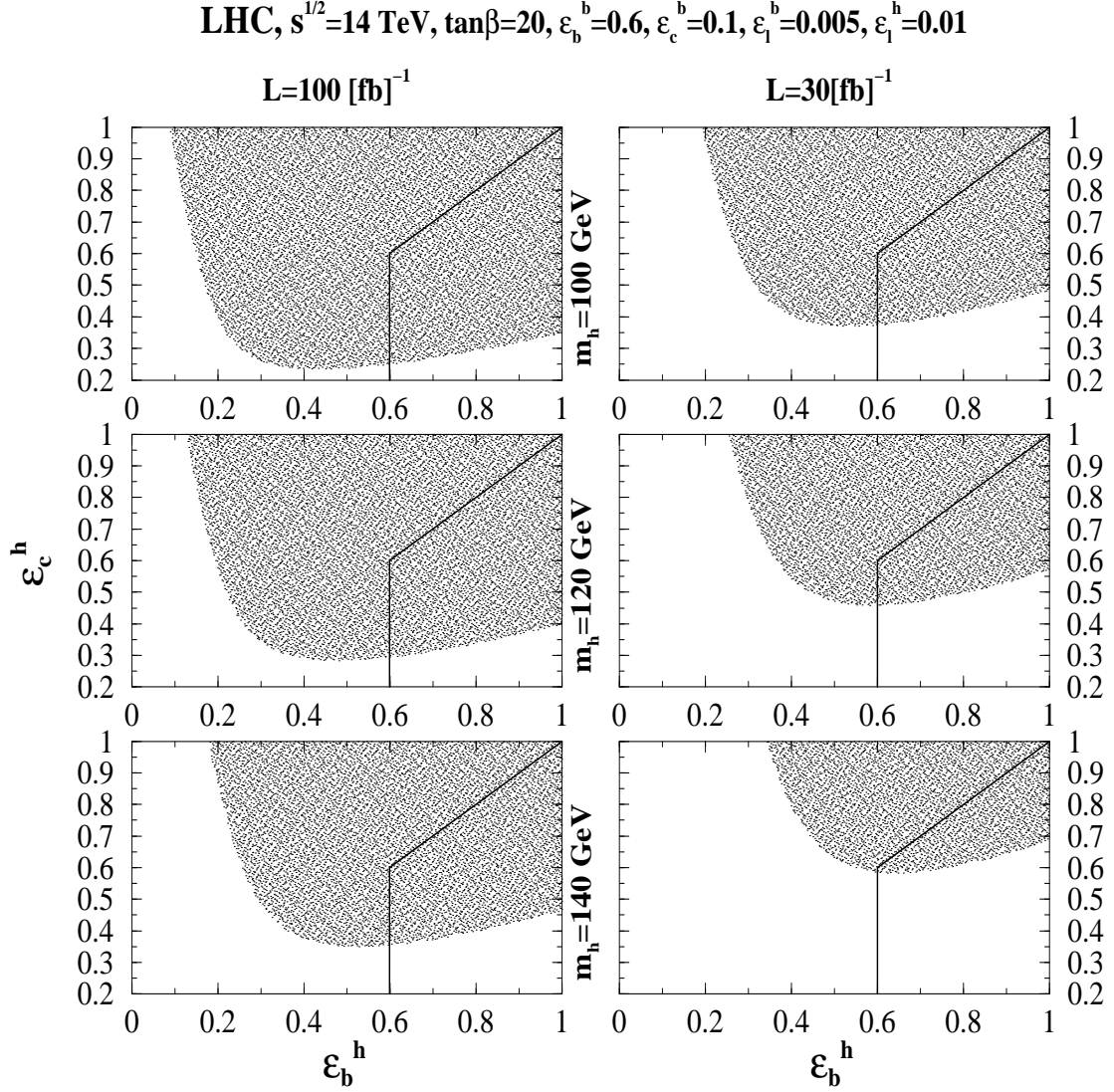


FIG. 3: Scatter plot for the LHC ($\sqrt{s} = 14$ TeV) in the $\epsilon_b^h - \epsilon_c^h$ plane, for $\tan\beta = 20$, $\epsilon_l^b = 0.005$, $\epsilon_l^h = 0.01$, $\epsilon_c^b = 0.1$ and $\epsilon_b^b = 0.6$. The shaded area allows an above 3-sigma detection of R^{T2HDM} at the LHC with integrated luminosity of 30 fb^{-1} (right column) and 100 fb^{-1} (left column) and for $m_h = 100$; 120 and 140 GeV on the first, second and third rows, respectively. The shaded area enclosed to the right of the solid lines corresponds to the conditions $\epsilon_b^h > \epsilon_c^h$ and $\epsilon_b^h > \epsilon_b^b$. All cross-sections were calculated for $\sigma_F = \sigma_R = m_h$ and with the set of cuts 1-4 as outlined in section III.

Yukawa potential in (15) by setting $U^1 = 0$ and $D^2 = 0$. Thus, in this model ϕ_2 is responsible for the mass generation of the up-type quarks while the down-type quark masses are generated through the VEV of ϕ_1 . Denoting again the three neutral Higgs species of the 2HDM II by h, H (the two CP-even scalars) and A (the CP-odd Higgs), their couplings to fermions are given by (see e.g., [13]):

$$\begin{aligned}
 hdd &: Y_d^{SM} [\sin(\alpha) \tan\beta \cos(\beta)] ; \\
 hu u &: Y_u^{SM} [\sin(\alpha) + \cot\beta \cos(\beta)] ; \\
 Hdd &: Y_d^{SM} [\cos(\alpha) + \tan\beta \sin(\beta)] ; \\
 Hu u &: Y_u^{SM} [\cos(\alpha) - \cot\beta \sin(\beta)] ; \\
 Add &: Y_d^{SM} \tan\beta \sin\alpha ;
 \end{aligned}$$

LHC, $s^{1/2}=14$ TeV, $\tan\beta=20$, $\varepsilon_b^b=0.4$, $\varepsilon_c^b=0.1$, $\varepsilon_l^b=0.005$, $\varepsilon_l^h=0.01$

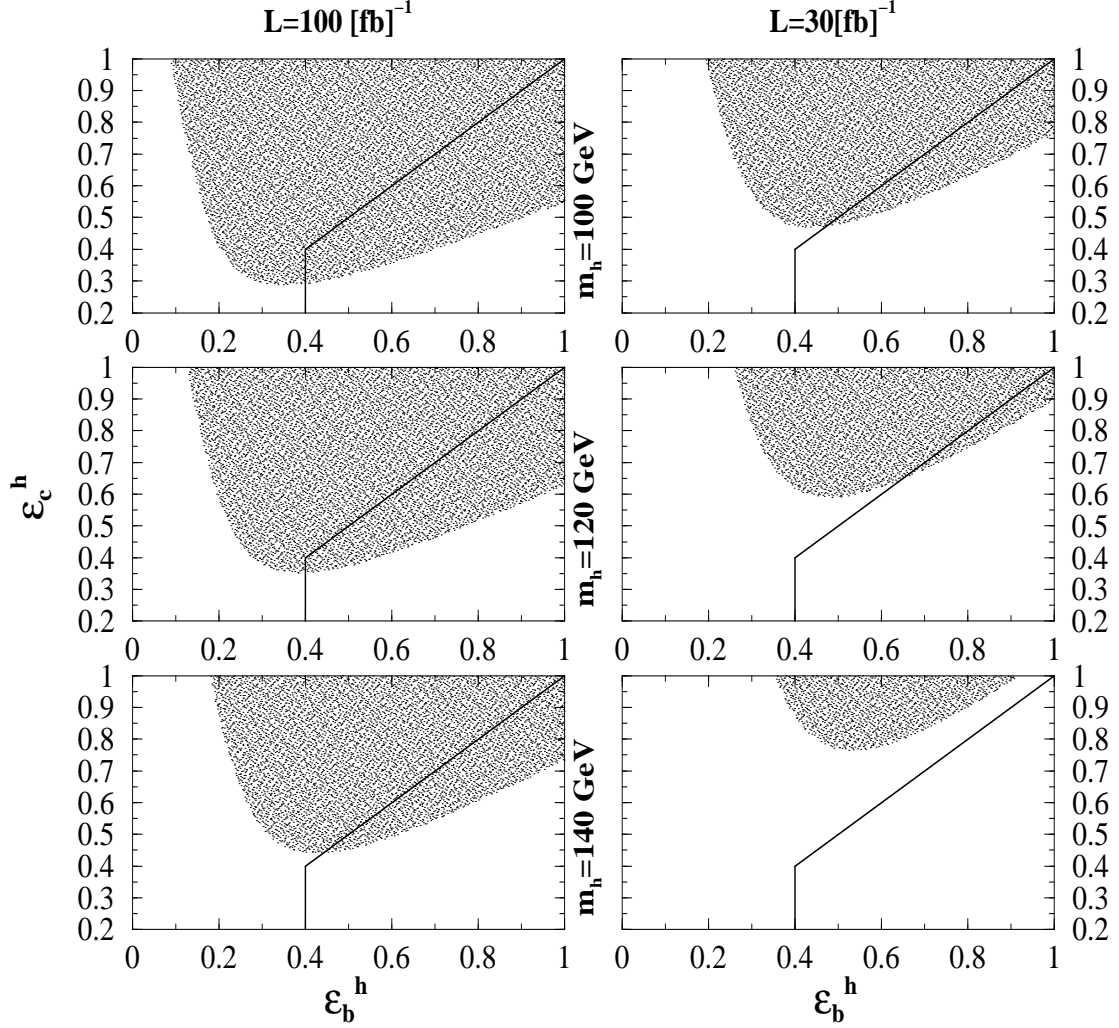


FIG. 4: Same as Fig. 3, for $\varepsilon_b^h = 0.4$.

$$A_{uu} : Y_u^{\text{SM}} \cot \beta ; \quad (18)$$

where $d(u)$ stands for a down (up) quark and β is the mixing angle in the CP-even Higgs sector. We will study three representative cases:

Case 1: $\cos(\beta) \neq 1$ or $\neq -1$.

Case 2: $\cos(\beta) \neq 0$ or $\neq \pm 1$.

Case 3: $\cos(\beta) = \sin(\beta) = 1/\sqrt{2}$ or $\neq 1/\sqrt{2}$.

The charm and bottom Yukawa couplings and their ratio, $Y_c=Y_b$, are given in Table V II, for the three cases

above and for each of the neutral Higgs bosons h, H and A .

The expected signals and their statistical significance for the three limiting cases and for the three neutral Higgs particles of the 2HDM II are compared to the T2HDM case in Table V III. Clearly, even in the more favorable cases in which $N_{\text{SD}}(2\text{HDM II}) = N_{\text{SD}}(\text{T2HDM}) = \tan^2 \beta$, the expected statistical significance in the 2HDM II case is still at least two orders of magnitude smaller than the one expected in the T2HDM when $\tan \beta > 10$. Therefore, based on the results ob-

TABLE VII: The charm and bottom Yukawa couplings Y_c and Y_b scaled by their SM Yukawa coupling Y_c^{SM} and Y_b^{SM} , respectively, and their ratio Y_c/Y_b in the 2HDM of type II. The Yukawa couplings of h , H and A are given for the three cases: (1) $\cos(\beta - \alpha) = 1$, (2) $\cos(\beta - \alpha) = 0$ and (3) $\cos(\beta - \alpha) = \sin(\beta - \alpha) = 1/\sqrt{2}$, see also text.

Y _c and Y _b in the 2HDM II				
Case	Higgs particle	Y_c/Y_c^{SM}	Y_b/Y_b^{SM}	Y_c/Y_b
1	h	$\frac{1}{\tan\beta}$	$\tan\beta$	$\frac{m_c}{m_b \tan^2\beta}$
	H	1	1	$\frac{m_c}{m_b}$
	A	$\frac{1}{\tan\beta}$	$\tan\beta$	$\frac{m_c}{m_b \tan^2\beta}$
2	h	$\frac{1}{\tan\beta}$	1	$\frac{m_c}{m_b}$
	H	$\frac{1}{\tan\beta}$	$\tan\beta$	$\frac{m_c}{m_b \tan^2\beta}$
	A	$\frac{1}{\tan\beta}$	$\tan\beta$	$\frac{m_c}{m_b \tan^2\beta}$
3	h	$\frac{1}{\tan\beta}$	$\frac{\tan\beta}{2}$	$\frac{m_c}{m_b \tan\beta}$
	H	$\frac{1}{\tan\beta}$	$\frac{\tan\beta}{2}$	$\frac{m_c}{m_b \tan\beta}$
	A	$\frac{1}{\tan\beta}$	$\tan\beta$	$\frac{m_c}{m_b \tan^2\beta}$

tained for the 2HDM scenario, we conclude that, no signal of R is expected to be observed at the LHC or at the Tevatron if the Yukawa Higgs sector is controlled by the 2HDM II. Hence, a measured signal of R at these hadron colliders will rule out the 2HDM II Higgs scenario with many standard deviations.

TABLE VIII: The expected 2HDM II signals, $R^{2\text{HDM II}}$, and their statistical significance, $N_{\text{SD}}^{2\text{HDM II}}$, scaled by the corresponding values in the 2HDM, for cases (1) $\cos(\beta - \alpha) = 1$, (2) $\cos(\beta - \alpha) = 0$ and (3) $\cos(\beta - \alpha) = \sin(\beta - \alpha) = 1/\sqrt{2}$, and for the three neutral Higgs of the model h , H and A .

Expected signals in the 2HDM II				
Case	Higgs particle	$\frac{R^{2\text{HDM II}}}{R^{2\text{HDM}}}$	$\frac{R^{2\text{HDM II}}_{\text{exp}}}{R^{2\text{HDM}}_{\text{exp}}}$	$\frac{N_{\text{SD}}^{2\text{HDM II}}}{N_{\text{SD}}^{2\text{HDM}}}$
1	h	$\frac{1}{\tan^4\beta}$	1	$\frac{1}{\tan^4\beta}$
	H	1	$\tan^2\beta$	$\frac{1}{\tan^2\beta}$
	A	$\frac{1}{\tan^4\beta}$	1	$\frac{1}{\tan^4\beta}$
2	h	$\frac{1}{\tan^4\beta}$	$\tan^2\beta$	$\frac{1}{\tan^2\beta}$
	H	$\frac{1}{\tan^4\beta}$	1	$\frac{1}{\tan^4\beta}$
	A	$\frac{1}{\tan^4\beta}$	1	$\frac{1}{\tan^4\beta}$
3	h	$\frac{1}{\tan^2\beta}$	1	$\frac{1}{\tan^2\beta}$
	H	$\frac{1}{\tan^2\beta}$	1	$\frac{1}{\tan^2\beta}$
	A	$\frac{1}{\tan^4\beta}$	1	$\frac{1}{\tan^4\beta}$

The 2HDM II Higgs framework also underlies the MSSM Higgs sector. However, due to the supersymmetric structure of the theory, the MSSM's Higgs sector is completely determined at tree-level by only two free parameters, conventionally chosen to be m_A and $\tan\beta$. That is, the mixing angle is fixed by m_A and $\tan\beta$ at tree level. Concentrating again on the large $\tan\beta$ case, in the MSSM one can distinguish two limiting cases:

Case 1: $m_A < m_h^{\text{max}}$, where $m_h^{\text{max}} = 120$ or 135 GeV, is the maximal allowed mass of the lighter CP-even Higgs after radiative corrections are included in the CP-even sector, depending whether one takes the minimal or the maximal stop mixing scenario, respectively [14]. In this case $\cos(\beta - \alpha) = 1$.

Case 2: $m_A^2 \gg m_Z^2$, the so called decoupling limit. In this limit $\cos(\beta - \alpha) = 0$.

These two MSSM limiting cases for large $\tan\beta$ remain valid also after the radiative corrections to the Higgs sector are included [15], thereby shifting the value of the mixing angle (the higher order contribution to $\tan\beta$, on the other hand, cause a large shift to the lighter CP-even Higgs mass, m_h).^[4] It should also be noted that, in the large $\tan\beta$ case, $\cos^2(\beta - \alpha)$ approaches zero very rapidly as m_A is increased. In particular, an order of magnitude drop of $\cos^2(\beta - \alpha)$ (from 1 to 0.1) is spanned over no more than about 10 GeV mass range of m_A [15].

Since cases 1 and 2 in the MSSM Higgs sector are equivalent to cases 1 and 2 of the 2HDM II framework, they have the same Yukawa couplings pattern as given in Table VII. Thus, applying the results obtained in the 2HDM II to the MSSM case, we conclude here too that R^{MSSM} cannot be observed either at the Tevatron or at the LHC. Reversing the argument, a measured signal of R at these hadron colliders will rule out the MSSM.

V. SUMMARY

To summarize, we have proposed a signal, R [see (1)], based on counting the number of three heavy (c or b) jets events versus the number of events with three b jets, in processes in which the neutral Higgs is produced in association with a single high p_T c or b jet. This signal assumes that the Higgs Yukawa coupling to the b quark is enhanced, say by a large $\tan\beta$ in multi-Higgs doublet models, and that the neutral Higgs will therefore be observed in association with b jets at future hadron collider experiments.

This signal was calculated in the framework of multi-Higgs models which have at least one neutral Higgs with an enhanced Yukawa coupling to the b quark when $\tan\beta$ is large. We have found that in such cases, the signal to background cross-section ratio is typically (after applying some useful kinematical cuts) $S/B = 0.1 - 1$ at the LHC and $S/B = 0.05 - 0.3$ at the Tevatron, depending on the value of $\tan\beta$.

The measurement of such a signal will require an efficiency for distinguishing a c jet from a light jet at the level

[4] There are also vertex corrections to the Higgs-fermion Yukawa couplings which do not depend on the mixing angle. However, these have a negligible effect in the up quark sector, and even more so for large $\tan\beta$ values [16].

of about $\frac{h_c}{c} = 20\%$, 30% or $\frac{h_c}{c} = 50\%$, 60% at the LHC or at the Tevatron, respectively. Such efficiencies seem to be somewhat higher than what has been attained in the simulations to date ($\frac{h_c}{c} = 10\%$) [17]. We have shown that if such c -jet tagging efficiencies are accomplished, then our signal will be very efficient for probing the ratio between the charm and bottom Yukawa couplings, $Y_c=Y_b$, thus allowing a deeper insight into the Higgs Yukawa potential. This, in turn, will be useful for categorizing the theory that underlies the Higgs sector. It should be noted, that our predictions for the Tevatron rely on an accumulated yearly luminosity of 30 inverse fb, which is, at present, considerably higher than the expected Fermilab's run II luminosity.

It should also be noted that the background estimate made for our signal was based on a low probability for misidentifying a light jet as a heavy jet, i.e., $\frac{b_1}{c_1} = O(1\%)$. While that value is comparable to the present estimate for $\frac{b_1}{c_1}$ (or even a little conservative), it is somewhat optimistic for $\frac{c_1}{b_1}$ which is not yet well studied by present detector simulations. A more realistic value for the distinction between a light jet and a charm jet, based on the technology of today, would be $\frac{c_1}{b_1} = O(10\%)$. Nonetheless, our background estimate (and therefore also our estimate for the significance of the signal) holds roughly for values of $\frac{c_1}{b_1}$ not larger than about 10%. For $\frac{c_1}{b_1}$ at the level of tens of percents there may well be other processes, e.g., $gg \rightarrow ggg$, that may alter our signal to background estimate to the level that the observability of our signal becomes difficult. Another potential problem to the detection of our signal may arise if the trigger algorithm

for b -jet tagging requires a minimum transverse momentum cut at the level of 100 GeV and above and the p_T cut of 30 GeV we used for the LHC and 15 GeV for the Tevatron proves to be too optimistic. In that case also, the signal proposed in this paper may be degraded and difficult to observe due to the large QCD background.

If the difficulties mentioned above can be summed out and such a signal is detected at the Tevatron or at the LHC, then the popular MSSM and the 2HDM II can be ruled out with many standard deviations, since in these theories the ratio $Y_c=Y_b$ is too small for our signal to have any measurable consequences. On the other hand, we have shown that within a version of a 2HDM – the “2HDM for the top” (T2HDM) – in which the large mass of the top quark is naturally accommodated for large $\tan\beta$, our signal can be easily observed at the LHC within the entire relevant mass range of the neutral Higgs if $\tan\beta > 20$ and $\frac{h_c}{c} = 20\%$, 30% . In addition, if the neutral Higgs of the T2HDM has a mass around 100 GeV and $\tan\beta > 50$, then our signal may also give an effect with more than 3-sigma significance at the Tevatron provided that $\frac{h_c}{c} = 50\%$, 60% .

Acknowledgments

We would like to thank F. Paige, W. Kilgore and S. Dawson for their helpful comments. G.E. also thanks the Technion President Fund. This work was also supported in part by US DOE Contract Nos. DE-FG 02-94ER 40817 (ISU) and DE-AC 02-98CH 10886 (BNL).

-
- [1] See e.g., D. Cavalli et al., in “Les Houches 2001, Physics at TeV Colliders”, R. Aurenche et al., IN2P3, Paris, France (2001), pp. 1-120, hep-ph/0203056; A. Djuadi, review talk given at the 7th Workshop on High-Energy Physics Phenomenology, WHEPP VII, Allahabad, India, January 4-15, 2002, Pramana 40, pp. 215-238 (2003), hep-ph/0205248; B. Mellado, for the CMS and ATLAS collaborations, talk given at the 14th Topical Conference on Hadron Collider Physics (HCP 2002), Karlsruhe, Germany, September 29 – October 4, 2002, Springer (2003), pp. 348-355, hep-ex/0211062.
- [2] D. Dicus, T. Stelzer, Z. Sullivan and S. Willenbrock, Phys. Rev. D 59, 094016 (1999); F. Maltoni, Z. Sullivan and S. Willenbrock, Phys. Rev. D 67, 093005 (2003); R. V. Harlander and W. B. Kilgore, hep-ph/0304035;
- [3] J. Campbell, R. K. Ellis, F. Maltoni and S. Willenbrock, Phys. Rev. D 67, 095002 (2003).
- [4] C. S. Huang and S. H. Zhu, Phys. Rev. D 60, 075012 (1999); J.-J. Cao, G.-P. Gao, Y.-L. Su and J. M. Yang, Phys. Rev. D 68, 075012 (2003);
- [5] J. Dai, J. F. Gunion and R. Vega, Phys. Lett. B 345, 29 (1995); J. Dai, J. F. Gunion and R. Vega, Phys. Lett. B 387, 801 (1996); E. Richter-Was and D. Froidevaux, Z. Phys. C 76, 665 (1997); J. L. Diaz-Cruz, H. J. He, T. Tait and C. P. Yuan, Phys. Rev. Lett. 80, 4641 (1998); C. Balazs et al., Phys. Rev. D 59, 055016 (1999); M. Carena, S. Mrenna and C. E. Wagner, Phys. Rev. D 60, 075010 (1999).
- [6] D. Choudhury, A. Datta and S. Raychaudhuri, hep-ph/9809552.
- [7] Comphep version 4.2.0 – a package for evaluation of Feynman diagrams and integration over multiparticle phase space. User's manual for version 3.3: A. Pukhov et al., hep-ph/9908288. URL: <http://theory.sinp.msu.ru/comphep>.
- [8] H. L. Lai et al., Eur. Phys. J. C 12, 375 (2000).
- [9] See e.g., J. A. M. Vermaseren, S. A. Larin and T. van Ritbergen, Phys. Lett. B 405, 327 (1997); H. Fusaoka and Y. Koide, Phys. Rev. D 57, 3986 (1998).
- [10] K. Hagiwara et al. (Particle Data Group), Phys. Rev. D 66, 010001 (2002).
- [11] See e.g., E. Richter-Was, D. Froidevaux and L. Poggioni, ATLAS Report No. ATL-PHYS-98-131; M. Sapinski (on behalf of the ATLAS collaboration), Eur. Phys. J. direct C 4S1, 08 (2002).
- [12] A. K. Das and C. Kao, Phys. Lett. B 372, 106 (1996); K. Kiers, A. Soni and G. H. Wu, Phys. Rev. D 59, 096001 (1999); G. H. Wu, and A. Soni, Phys. Rev. D 62, 056005 (2000); K. Kiers, A. Soni and G. H. Wu, Phys. Rev. D 62, 116004 (2000).
- [13] For reviews on the Higgs sector in the Standard Model, the two Higgs doublet model and in supersymmetry, see

- e.g., J. Gunion, H. Haber, G. Kane and S. Dawson, "The Higgs Hunters Guide", Addison-Wesley, Reading 1990; D. Atwood, S. Bar-Shalom, G. Eilam and A. Soni, Phys. Rep. 347, 1 (2001).
- [14] See e.g., J.R. Espinosa and R.-J. Zhang, Nucl. Phys. B 586, 3 (2000); S. Heinemeyer, W. Hollik and G. Weiglein, hep-ph/0002213.
- [15] See e.g., J.F. Gunion, H.E. Haber and R. van Kooten, hep-ph/0301023 and references therein.
- [16] See e.g., M. Carena, H.E. Haber, H.E. Logan and S. Mrenna, Phys. Rev. D 65, 055005 (2002) and references therein.
- [17] F. Paige and W. Kilgore, private communications.